Full length article

Mechanism study on a new antimicrobial peptide Sphistin derived from the N-terminus of crab histone H2A identified in haemolymphs of *Scylla paramamosain*

CrossMark

Bei Chen [a, 1], Dan-Qing Fan [a, 1], Ke-Xin Zhu [a], Zhong-Guo Shan [a], Fang-Yi Chen [a], Lin Hou [a], Ling Cai [a], Ke-Jian Wang [a, b, c, *]

[a] State Key Laboratory of Marine Environmental Science, College of Ocean & Earth Science, Xiamen University, Xiamen, Fujian 361102, PR China
[b] Fujian Collaborative Innovation Center for Exploitation and Utilization of Marine Biological Resources, Xiamen University, Xiamen, Fujian 361102, PR China
[c] Fujian Engineering Laboratory of Marine Bioproducts and Technology, Xiamen University, Xiamen, Fujian 361102, PR China

ARTICLE INFO

ABSTRACT

Histone H2A is known to participate in host immune defense through generating special antimicrobial peptides (AMPs), for which it has been an interesting research focus to characterize this kind of peptides in vertebrates and invertebrates. Although thousands of AMPs have been reported in variety of life species, only several AMPs are known in crabs and in particular no H2A-derived AMP has yet been reported. In the present study, a 38-amino acid peptide with antimicrobial activity was determined based on the sequence analysis of a histone H2A identified from the mud crab *Scylla paramamosain*. The histone H2A derived peptide was an AMP-like molecule and designated as Sphistin. Sphistin showed typical features of AMPs such as amphiphilic α-helical second structrue and positive charge net. The synthetic Sphistin exerted high antimicrobial activity against Gram-positive, Gram-negative bacteria and yeast, among which *Aeromonas hydrophila*, *Pseudomonas fluorescens* and *Pseudomonas stutzeri* are important aquatic pathogens. Leakage of the cell content and disruption of the cell surface were observed in bacterial cells treated with Sphistin using scanning electron microscopy. It was proved that the increasing cytoplasmic membrane permeability of *Escherichia coli* was caused by Sphistin. Further observation under confocal microscopy showed that Sphistin could combine onto the membrane of *Staphylococcus aureus*, *E. coli* MC1061 and *Pichia pastoris* but not translocate into the cytoplasm. Moreover, the affinity of Sphistin with either LPS or LTA was also testified that there was an interaction between Sphistin and cell membrane. Thus, the antimicrobial mechanism of this peptide likely exerted via adsorption and subsequently permeabilization of the bacterial cell membranes other than penetrating cell membrane. In addition, synthetic Sphistin exhibited no cytotoxicity to primary cultured crab haemolymphs and mammalian cells even at a high concentration of 100 μg/mL for 24 h. This is the first report of a histone-derived Sphistin identified from *S. paramamosain* with a specific antimicrobial activity and mechanism, which could be a new candidate for future application in aquaculture and veterinary medicine.

© 2015 Elsevier Ltd. All rights reserved.

1. Introduction

Histones are traditionally known as the principal protein component of chromatin [1]. In the past decade, many observations suggest that histones are involved in a multitude of biological functions beyond the confines of the nuclear envelope [2]. For instance, the histone can act as endotoxin-neutralizing proteins [3,4], leucocytes stimulatory factor [5], homeostatic thymus hormone [6] as well as apoptotic signal transmitting factor [7] and also

as an antimicrobial peptide.

Since the antimicrobial activity of histones was firstly reported in 1932, histone-derived antimicrobial peptides across almost all kind of histones (histone H1, H2A, H2B, H3, and H4) have been discovered to display antimicrobial activities against bacteria, fungi, viruses and protozoa. Previous studies show that histone-derived peptides from various vertebrates, such as mammals [3,8–11], chicken [12], frog [13] and fish [14–20], all possess antimicrobial activity. Meanwhile a few studies have reported that this class of antimicrobial peptides is also identified in invertebrates, such as histone H2A fragments in scallop (*Chlamys farreri*) [21], abalone (*Haliotis discus discus*) [22], Pacific white shrimp (*Litopenaeus vannamei*) [23] and freshwater prawn (*Macrobrachium rosenbergii*) [24,25].

Some histone antimicrobial peptides are found to be a extra-cellular secreted antimicrobial peptide, which are purified from skin or epithelium and derived from intact histone precursors through proteolytic cleavage [26,27]. The active histone fragments are usually derived from the N-terminal part of histone. For instance, buforin I, isolated from the stomach extract of the Korean frog *Bufo bufo gargarizans*, is processed from unacetylated histone H2A by pepsin C isozymes [26]. Parasin I, isolated from the skin mucus secretions of channel catfish, is the fragmented histone processed by cathepsin D [27]. In addition to endogenous histones, synthetic and recombinant histone-derived N-terminal fragments also display potent bacterial killing activity. The reported Abhisin, a potential antimicrobial peptide derived from histone H2A of disk abalone (*H. discus discus*), is synthesized and shows antimicrobial and anticancer activity [22]. The N-terminal fragment of scallop (*C. farreri*) histone H2A peptide is expressed in *Pichia pastoris* GS115 and exerts antibacterial activity against both Gram-positive and Gram-negative bacteria [21]. Thus N-terminus of histone H2A could be an active antimicrobial peptide.

The mud crab, *Scylla paramamosain*, is an important fisheries and aquaculture species in China. As to other invertebrates, antimicrobial peptides (AMPs) play crucial roles in the natural defense system against microbial invasion in the crab. So far there are some AMPs identified in several crab species, including linear α-helical AMPs Bac-like [28] and Callinectin [29], anionic AMPs Scygonadin [30], cysteine-rich AMPs ALFs [31], Multi-domain or chimeric AMPs Crustin Hyastatin [32], Arasin [33] and GRPSp [34]. However, no histone-derived AMP has been reported and its antimicrobial mechanism is still unknown in crab so far. In the present study, based on the determined gene sequence of histone H2A in the mud crab *S. paramamosain*, a 38 aa N-terminal peptide was identified and named as Sphistin. To understand the antimicrobial activity of Sphistin, a synthetic Sphistin peptide was produced and its spectrum of activity against bacteria and yeast was measured. The bacterial binding assay and membrane integrity assay were carried out to understand its antimicrobial mechanism. The LPS and LTA binding experiment was designed in order to know the possibility of intereaction between Sphistin and negatively charged molecules located on the bacterial surface. Finally, the cytotoxicity of Sphistin on normal cells was investigated. From the study, the antimicrobial properties and mechanism of this new histone-derived antimicrobial peptide in carb will be evaluated and thus would further shed light on the innate immune system of crustaceans.

2. Materials and methods

2.1. Determination of histone H2A cDNA and genomic DNA sequences

In our previous study, a forward suppression subtractive hybridization (SSH) cDNA library was constructed from haemolymphs of *S. paramamosain* and the up-regulated genes were identified in order to isolate differentially expressed genes in response to LPS [35]. Partial sequence of mud crab histone H2A was identified during the screening of the SSH cDNA library database.

RACE PCR was performed to amplify the full-length histone H2A cDNA sequence. Specific primers were designed according to the obtained partial cDNA sequence (Table 1). RACE cDNA was prepared with an SMART RACE cDNA Amplification kit (Clontech) and was used as template for PCR. PCR conditions were as follows: 94 °C for 4 min, 35 cycles of 94 °C for 30 s, 60 °C for 30 s and 72 °C for 30 s. The final extension was carried out at 72 °C for 10 min.

Total genomic DNA was prepared from the carb muscle using MiniBEST Animal Tissue Genomic DNA Extraction Kit Ver.2.0 (Takara). The genomic sequence of histone H2A was amplified by PCR reaction using primers intron F and R (Table 1), and the LA Taq DNA polymerase (Takara). The amplification conditions were: 1 min at 94 °C, 35 cycles of 10 s at 98 °C, 4 min at 68 °C, then 10 min at 72 °C for further extension.

All the expected DNA fragment was ligated to pMD18-T vector (Takara) and transformed into *Escherichia coli* DH5α. Positive clones were identified by bacterial-colony PCR and sequenced.

2.2. Sequence analysis

Nucleotide and deduced amino acid sequences of Histone H2A cDNA were analyzed using software DNAsis. The calculated molecular mass and the theoretical isoelectric point were predicted by SIB Bioinformatics Resource Portal (http://web.expasy.org/compute_pi/). Signal peptide was predicted by SignalP 4.0 Server (http://www.cbs.dtu.dk/services/SignalP/). Protein sequences of Histone H2A from different organisms were obtained through the NCBI BLAST search program. A multiple sequence alignment was created with software Bioedit. Phylogenetic trees of the selected Histone H2A was constructed using the neighbour-joining method, and the reliability of the branching was tested using bootstrap resampling (with 1000 pseudo-replicates). The figure was drawn using the MEGA5. The gemonic sequence of Histone H2AZ from different organisms was obtained through the NCBI and a schematic representation of the exon and intron organization was drawn by DNAMAN8. The α-helical secondary structure was predicted using the DNAstar Protean program and helical wheel modeling. Moreover, the 3D structure of Sphistin was also predicted in http://swissmodel.expasy.org/interactive.

2.3. Synthesis of the Sphistin peptide sequence

A 38 aa sequence of Sphistin peptide. (MAGGKAGKDSGKAKA-KAVSRSARAGLQFPVGRIHRHLK) which was derived from the N-terminus of the mud crab histone H2A was synthesized using the solid phase peptide synthesis method (TASH Co., China). The molecular masses and purity of the purified peptides were verified by mass spectroscopy and HPLC, respectively.

2.4. Microorganisms

All strains were purchased from the CGMCC with the exception of *E. coli* MC1061 and the yeast strain *P. pastoris* GS115, which were kindly provided by Dr. Chun Li and bought from Invitrogen Biotech respectively. The bacteria were cultured overnight at the appropriate temperature (28 °C or 37 °C) either on Muller-Hinton agar or marine agar 2216 (Difco). Yeast strains were grown on YPG agar (yeast extract 1%, peptone 1%, and glucose 2%) at 28 °C for 2 d for the experiments.

Table 1
Sequences of primers used in this study.

Application	Primer sequence	GenBank ID or Ref.
3′ RACE	5′-CCAAAGACTTGAAGGTGAAGCGTAT-3′	FJ774663
Intron	F 5′-AACAGTGGTAGCGAGTGCAGG-3′	FJ774663
	R 5′-CACCTCAGCCCATCACTGACGTAC-3′	
TNF super family (TNFSF)	F 5′-CTGTTGTACGTCAGGTCGACTCT-3′	Transcriptome
	R 5′-GGCTCTTCGTATGGGACCTCTG-3′	
TNF receptor super family (TNFRSF)	F 5′-GAACCGGTCTGTTGAGTCACAG-3′	Transcriptome
	R 5′-GCTCAGAACGCCTGTGTTGTC-3′	
LPS-induced TNF-α factor (LITAF)	F 5′-TGCAGTGTGGGCAGCTATGTTC-3′	Transcriptome
	R 5′-AGGCTGGTGCTCCAACAACTGT-3′	
Spätzle	F 5′-CTGGGCAGAACACACAGGAGTCT-3′	Transcriptome
	R 5′-GTACGATGAGCGGATCAAGCAGC-3′	
Crustin	F 5′-ACCTGCCTTTACCAACGGCTT-3′	EU161287
	R 5′-CAACAGTCTTGCATACGTGGTGC-3′	
ALF2	F 5′-GGACGCCATCAAGGACTTCGT-3′	JQ069031
	R 5′-CATCCATTACAGGTCAGACACGAG-3′	
β-actin	F 5′-GCCCTTCCTCACGCTATCCT-3′	GU992421
	R 5′-GCGGCAGTGGTCATCTCCT-3′	

2.5. Antimicrobial assays

Antimicrobial activity was evaluated by measuring minimum inhibitory concentration (MIC) values which was described by Bulet et al. [36]. Briefly, dilutions of the synthetic Sphistin with 10 mM NaPB (pH 7.7) were proceeded to obtain a series of final concentrations from 1.5 μM to 48 μM. About 10^4 CFU of bacteria/well and 10^3 CFU of yeast/well were incubated with serial dilutions of synthetic peptide in the presence of appropriate growth media. Samples without Sphistin were used as blanks. After 24 h (48 h for yeast) of incubation at 28 °C, MIC was calculated as the lowest peptide concentration yielding no detectable growth. The aliquots of the cultures were then plated on appropriate agar and MBC was the concentration which killed more than 99.9% microorganisms after incubation at either 37 °C or 28 °C. This assay was performed in triplicate.

Kinetics of bactericidal activity was performed using *Corynebacterium glutamicum*, *Staphylococcus aureus* and *E. coli* MC1061 as described by Tencza et al. [37]. Synthetic Sphistin at the concentration of MBC (1.5 μM, 3 μM and 25 μM) was incubated with *C. glutamicum*, *S. aureus* and *E. coli* MC1061 respectively. The procedure was the same as described in the antimicrobial assay. At each time point of incubation, 8 μL bacteria diluent and synthetic Sphistin mixtures was taken to dilute in 10 mM NaPB and plated on nutrition broth agar. The percentages of the recovered bacterial CFU in each time point to the initial CFU (with peptide) was calculated and plotted.

2.6. Morphological observation by SEM

Scanning electron microscopy (SEM) was conducted to evaluate the antibacterial mechanism of Sphistin. A high concentration of supra-MBC of peptide was chosen in order to achieve killing of a high number of bacteria cells. *S. aureus*, *E. coli* MC1061 or *P. pastoris* GS115 were prepared in 0.1 M NaPB buffer (final concentration of 5×10^8 cfu/mL) and incubated with synthetic Sphistin peptide at 28 °C for 15 min, 40 min and 1 h respectively. They were fixed with 2.5% glutaraldehyde in 0.1 M NaPB (pH 7.4) for 3 h. After washing, the bacteria precipitate were resuspended and allowed to adhere to poly-L-lysine-coated slides for 30 min on ice. The slides were subsequently dehydrated with a graded ethanol series and tertiary butanol. The samples were lyophilized, coated with gold in an ion coater, and examined by scanning electron microscopy on an FEI XL-30 Environmental Scanning Electron Microscope.

2.7. Membrane integrity assay

In order to explore the mechanism that synthetic Sphistin peptide effected to the bacteria, a real-time membrane integrity assay was performed as the previous studies [38–40]. *E. coli* MC1061 constitutively expresses recombinant luciferase. The perforation of the plasma membrane caused influx of externally added D-luciferin and resulted in light emission. In the study, 50 μL of MH medium containing 1.0×10^7 CFU *E. coli* cells MC1061 and 2 mM D-luciferin (10 mM Tris–HCl buffer, pH 7.4) was mixed with 50 μL dilution of the peptide with final concentration of 25 μM and 50 μM (corresponding to the $1 \times$ MBC and $2 \times$ MBC). Luminescence was monitored using an Envision HTS microplate reader (Tecan). The cecropin P1 (Sigma) and Argireline (TASH Co., China) were employed as control peptides. All measurements were repeated at least three replicates.

2.8. Confocal microscopy imaging of bacteria

The preparation of bacteria was similar with scanning electron microscopy invegation. Briefly, *S. aureus*, *E. coli* MC1061 and *P. pastoris* were adjusted to 1×10^9 cfu/mL and exposed to synthetic Sphistin peptide for 30 min at 28 °C. After fixation and washing, bacteria cell were placed on a poly-L-lysine coated glass slide and surrounded with a hydrophobic barrier pen. The slides were then washed by PBS and followed by permeabilization in 0.1% Triton X-100 buffer at room temperature for 10 min. For immunostaining, bacteria cells were blocked with 10% goat serum at room temperature for 2 h and added with rabbit polyclonal anti-N-terminal H2AFV antibody (1:100 dilution, ABGENT) at 4 °C overnight. The cells were then washed and incubated with DyLight649-conjugated Goat anti-rabbit antibodies (1:800 dilution, MULTISCIENCES) at room temperature for 1 h. Finally stained the cell with DAPI (0.5 μg/ml). We recorded images on a Zeiss LSM 780 MultiPhoto Laser Scanning Microscopy.

2.9. Binding property to bacterial associated components

The binding properties to bacterial associated components of Sphistin were investigated by ELISA as described previously by Gonzalez et al. [41] and Zhang Qiuxia et al. [42]. Briefly, LPS (from *E. coli* 055:B5, Sigma) or LTA (from *S. aureus*, Sigma) were prepared in 100 mM Na_2CO_3, 20 mM EDTA, pH 9.6 and 3 μg/well coated on the microtiter plate for 2 h at 60 °C. After washing away the redundant LPS or LTA, the coated plates were blocked with 5% (w/v)

BSA/PBS for 1 h at room temperature. Then the serial dilution of the synthetic Sphistin protein (0–150 μg/mL, 100 μL/well) was incubated for 1 h at room temperature. After washing the excess protein with PBS buffer containing 0.05% Tween 20, the ELISA plate was hybridized with the rabbit anti-H2AFV antibody (1:1000 dilution, 50 μL/well, ABGENE) for 2 h at 37 °C. The samples were washed as above and followed by incubation with HRP-labeled Goat Anti-rabbit IgG (1:1000 dilution, 50 μL/well) at 37 °C for 1 h. Then, 100 μl of TMB substrate solution was added and incubated at room temperature for 15–30 min in the dark. Finally, Add 50 μl of 1 M H_2SO_4 to stop the reaction and read the absorbance at 450 nm by Tecan Infinite F200 PRO multiscan plate reader. The results from four experiments were used for statistical analysis. The binding results were analyzed by Scatchard plot analysis. The binding parameters, apparent dissociation constant Kd, and the maximum binding (Amax), were determined by non-linearly fitting as $A = Amax[L]/(Kd + [L])$, where A was the absorbance at 450 nm and [L] was the protein concentration.

2.10. Determination of cytotoxicity effect of synthetic Sphistin peptide

The cytotoxicity of Sphistin was evaluated on the mouse osteoblastic cell line (MC3T3-E1) and crab haemolymph. MC3T3-E1 cells were cultured in α-MEM supplemented with 5% FBS, 100 μg/mL penicillin and 100 IU/mL streptomycin (Gibco) in 5% CO_2 humidified incubator at 37 °C. Crab haemolymphs were collected and cultured as described previously by Dingjian et al. [43]. Briefly, haemolymphs (5×10^6 cells/mL) were seeded in Leibovitz L-15 medium (Hyclone) containing 5% FBS (Gibco), 100 IU/mL penicillin, 100 μg/mL streptomycin and 0.12 g/L NaCl at 20 °C. 100 μL of MC3T3-E1 and crab haemolymph were seeded in 96 well plates overnight and then incubated with 0, 25, 50, 100 μg/mL synthetic Sphistin for 24 h. Samples in wells containing only media were maintained as controls. The cell viability was determined using the CellTiter 96 Aqueous Non-Radioactive Cell Proliferation Assay (Promega). After 20 μL of the MTS/PMS reagent was added to each well, the cells were incubated for 2 h or 6 h, respectively. The absorbance of each well was measured at 490 nm in a microplate reader (Tecan). Cell viability percentage (%) was calculated for each concentration relative to control cells and data were the means of a minimum of three replicates.

2.11. Immunomodulatory activities of synthetic Sphistin peptide

The effect of Sphistin on the expression profile of immune-related gene in crab haemolymph was detected by qPCR. The haemolymphs were cultured in absence or presence of Sphistin (25 μg/mL) for 3, 6, 12 and 24 h. Hemocyte pellets were preserved in Trizol reagent (Invitrogen) for RNA extraction. The total RNA isolation and cDNA synthesis (Takara) were performed following the manufacturer's instructions. Real-time PCR was performed with the ABI Prism 7500 instrument (Applied Biosystems) using FastStart Universal SYBR Green Master (Rox) (Roche). Reaction mixtures were incubated for 2 min at 50 °C, 10 min at 95 °C, followed by 40 cycles of 15 s at 95 °C, 1 min at 60 °C. The relative transcript levels were corrected by normalization based on the housekeeping gene β-actin transcript levels. All primers used were listed in Table 1. GenBank accession numbers for the gene sequences used in the present study are as follows: ALF2 (JQ069031), Crustin (EU161287), β-actin (GU992421). While the sequences of Spätzle, TNFSF, TNFRSF and LITAF were obtained from the embryonic transcriptome of S. paramamosain (unpublished data).

3. Results

3.1. Identification and characterization of the cDNA sequence of histone H2A from mud crab

The cDNA sequence and deduced amino acid sequences of the mud crab histone H2A are shown in Fig. 1. It contained 1096 bp including 28 bp in the 5′ untranslated region (UTR), an open reading frame (ORF) of 387 bp, and a 681 bp in the 3′ UTR, in which a putative imperfect polyadenylation signal AATATA appeared between the stop codon (TAA) and the poly (A) tail.

The open reading frame encodes a 128 amino acid peptide. No signal peptide was predicted in the N-terminus. The calculated molecular mass of the protein was 13.4 kDa with an estimated isoelectric point of 10.58. And a typical signature domain (^{24}AGLQFPV^{30}) of histone H2A was predicted. Histone H2A nucleotide sequence has been deposited in the GenBank under accession number FJ774663.

Six H2A variants have been found in commonly studied species, H2A.1, H2A.2, H2A.X, H2A.Z, MacroH2A (MacroH2A1, MacroH2A2) and H2AB (H2A.Lap1, H2A.Bbd) [44,45]. Phylogenetic relationship analysis revealed that mud crab H2A sequence was grouped into the group of histone H2A.Z and was in the same branch position with invertebrates H2A.Z, as shown in the Fig. 2. Despite the evolutionary divergence of vertebrates and invertebrates for H2A.Z, the protein sequences of histone H2A.Z are remarkably conserved. The identity of amino acid sequence deduced from mud crab histone H2A was 100%, 99%, 96%, 95% and 96% with Apis florea (XP_003693090.1), Mytilus galloprovincialis (AEH58058.1), Cyprinus carpio (AFV36373.1), Gallus gallus (NP_001026545.1) and Homo sapiens (NP_002097.1) histone H2A like protein, respectively, based on the BLASTp results. Comparative cDNA sequence analysis of the histone H2A, mud crab histone H2A has 82% and 79% identity with Pagrus major (AY190700.1) and Gallus gallus (NM_001031374.1), respectively.

3.2. Analysis of gene organization

The full-length of mud crab histone H2A genomic DNA consisted of 2767 bp. The gene organization of mud crab histone H2A were compared with that of other species reported in the NCBI GenBank database: Mus musculus (NC_000069.6), H. sapiens (L10138.1), Xenopus tropicalis (NW_004668232.1) and Drosophila melanogaster (NT_033777.3). The position and relative size of exons and introns are drawn to scale as shown in Fig. 3. The schematic representation of gene organization comparison indicated that almost all of the histone H2A.Z genomic DNA possess an identical 5-exons/4-introns organization except for mud crab histone H2A consisted of 3 introns and 4 exons. We also observed that the both the size of the second and third exon being highly conserved among various species, respectively.

3.3. Identification and characterization of the Sphistin sequence from histone H2A

A multiple sequence alignment of histone H2A-derived AMP was proceeded and the details was shown in the Fig. 4. The N-terminal domain of mud crab histone H2A has significant similarity with histone-derived AMPs such as buforin I, hipposin and abhisin. With reference to the previous reports, the 38 amino acids at the N-terminus of Sphistin were predicted by Antimicrobial Peptide Predictor (http://aps.unmc.edu/AP/prediction/prediction_main.php). It showed typical features of AMPs including higher positive charge (+9), total hydrophobic ratio (36%) and a protein-binding potential of 2.11 kcal/mol. Therefore, the part peptide
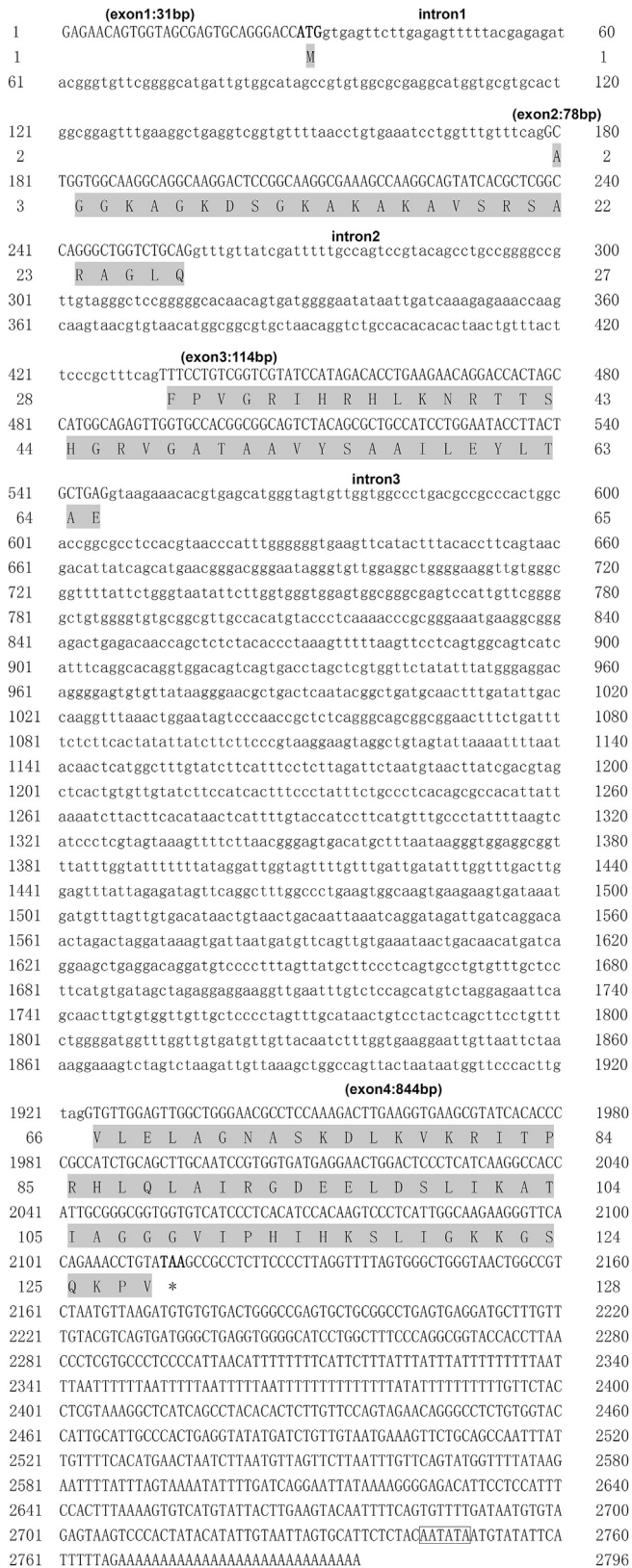
```
  1   GAGAACAGTGGTAGCGAGTGCAGGGACCATGgtgagttcttgagagtttttacgagagat    60
  1                                 M                                 1

 61   acgggtgttcggggcatgattgtggcatagccgtgtggcgcgaggcatggtgcgtgcact   120
                                          (exon2:78bp)
121   ggcggagtttgaaggctgaggtcggtgttttaacctgtgaaatcctggtttgtttcagGC   180
  2                                                              A     2
181   TGGTGGCAAGGCAGGCAAGGACTCCGGCAAGGCGAAAGCCAAGGCAGTATCACGCTCGGC   240
  3    G  G  K  A  G  K  D  S  G  K  A  K  A  K  A  V  S  R  S  A      22
                            intron2
241   CAGGGCTGGTCTGCAGgtttgttatcgattttttgccagtccgtacagcctgccggggccg   300
 23    R  A  G  L  Q                                                  27
301   ttgtagggctccgggggcacaacagtgatggggaatataattgatcaaagagaaaccaag   360
361   caagtaacgtgtaacatggcggcgtgctaacaggtctgccacacacactaactgtttact   420
                         (exon3:114bp)
421   tcccgctttcagTTTCCTGTCGGTCGTATCCATAGACACCTGAAGAACAGGACCACTAGC   480
 28               F  P  V  G  R  I  H  R  H  L  K  N  R  T  T  S       43
481   CATGGCAGAGTTGGTGCCACGGCGGCAGTCTACAGCGCTGCCATCCTGGAATACCTTACT   540
 44    H  G  R  V  G  A  T  A  A  V  Y  S  A  A  I  L  E  Y  L  T      63
                     intron3
541   GCTGAGgtaagaaacacgtgagcatgggtagtgttggtggccctgacgccgcccactggc   600
 64    A  E                                                           65
601   accggcgcctccacgtaacccatttgggggggtgaagttcatactttacaccttcagtaac   660
661   gacattatcagcatgaacgggacgggaataggggtgttggaggctgggaaggttgtgggc   720
721   ggttttattctgggtaatattcttggtgggtggagtggcgggcgagtccattgttcgggg   780
781   gctgtgggggtgtgcggcgttgccacatgtaccctcaaaacccgcgggaaatgaaggcggg   840
841   agactgagacaaccagctctctacaccctaaagtttttaagttcctcagtggcagtcatc   900
901   atttcaggcacagtgtgacagtcagtagctcgtcgttggttcctctatatttatggggagac   960
961   agggggagtgttattaagggaacgctgactcaatacggctgatgcaacttgatattgac  1020
1021  caaggtttaaactggaatagtcccaacccgctctcagggcagcggcggaactttctgattt  1080
1081  tctcttcactatattatcttcttcccgtaaggaagtaggctgtagtattaaaattttaat  1140
1141  acaactcatggctttgtatcttcatttcctcttagattctaatgtaacttatcgacgtag  1200
1201  ctcactgtgttgtatcttccatcactttccctatttctgccctcacagcgccacattatt  1260
1261  aaaatcttacttcacataactcattttgtaccatccttcatgtttgccctattttaagtc  1320
1321  atccctcgtagtaaagttttcttaacgggagtgacatgtcttttaataaaggtggaggcggt  1380
1381  ttatttggtatttttttataggattggtagttttgtttgattgatatttggtttgacttg  1440
1441  gagtttattagagatagttcaggctttggccctgaagtggcaagtgaagaagtgataaat  1500
1501  gatgtttagttgtgacataactgtaactgacaattaaatcaggatagattgatcaggaca  1560
1561  actagactaggataaagtgattaatgatgttcagttgtgaaataactgacaacatgatca  1620
1621  ggaagctgaggacaggatgtccccttttagttatgcttccctcagtgcctgtgtttgctcc  1680
1681  ttcatgtgatagctagaggaggaaggttgaatttgtctccagcatgctctaggagaattca  1740
1741  gcaacttgtgttggttgttgctcccctagtttgcataactgtcctactcagcttcctgttt  1800
1801  ctgggatggtttggtttgtgatgttgttacaatctttggtgaaggaattgttaattctaa  1860
1861  aaggaaagtctagtctaagattgttaaagctggccagttactaataatggttcccacttg  1920
                                                        (exon4:844bp)
1921  tagGTGTTGGAGTTGGCTGGGAACGCCTCCAAAGACTTGAAGGTGAAGCGTATCACACCC  1980
 66      V  L  E  L  A  G  N  A  S  K  D  L  K  V  K  R  I  T  P       84
1981  CGCCATCTGCAGCTTGCAATCCGTGGTGATGAGGAACTGGACTCCCTCATCAAGGCCACC  2040
 85    R  H  L  Q  L  A  I  R  G  D  E  E  L  D  S  L  I  K  A  T     104
2041  ATTGCGGGCGGTGGTGTCATCCCTCACATCCACAAGTCCCTCATTGGCAAGAAGGGTTCA  2100
105    I  A  G  G  G  V  I  P  H  I  H  K  S  L  I  G  K  K  G  S     124
2101  CAGAAACCTGTATAAGCCGCCTCTTCCCCTTAGGTTTTAGTGGGCTGGGTAACTGGCCGT  2160
125    Q  K  P  V  *                                                 128
2161  CTAATGTTAAGATGTGTGTGACTGGGCCGAGTGCTGCGGCCTGAGTGAGGATGCTTTGTT  2220
2221  TGTACGTCAGTGATGGGCTGAGGTGGGGCATCCTGGCTTTCCCAGGCGGTACCACCTTAA  2280
2281  CCCTCGTGCCCTCCCCATTACATTTTTTTTCATTCTTTATTTATTTATTTTTTTTTAAT  2340
2341  TTAATTTTTAATTTTTAATTTTTAATTTTTTTTTTTTTTTATATTTTTTTTTTGTTCTAC  2400
2401  CTCGTAAAGGCTCATCAGCCTACACACTCTTGTTCCAGTAGAACAGGGCCTCTGTGGTAC  2460
2461  CATTGCATTGCCCACTGAGGTATATGATCTGTTGTAATGAAAGTTCTGCAGCCAATTTAT  2520
2521  TGTTTTCACATGAACTAATCTTAATGTTAGTTCTTAATTTGTTCAGTATGGTTTTATAAG  2580
2581  AATTTTATTTAGTAAAATATTTTGATCAGGAATTATAAAAGGGGAGACATTCCTCCATTT  2640
2641  CCACTTTAAAAGTGTCATGTATTACTTGAAGTACAATTTTCAGTGTTTTGATAATGTGTA  2700
2701  GAGTAAGTCCCACTATACATATTGTAATTAGTGCATTCTCTACAATATAATGTATATTCA  2760
2761  TTTTTAGAAAAAAAAAAAAAAAAAAAAAAAAAAAAAAA                         2796
```

Fig. 1. Genomic DNA, cDNA and the predicted amino acid sequence of the mud crab histone H2A cDNA. The cDNA sequence has been deposited in GenBank under accession number FJ774663. The start (ATG) and stop (TAA) codons are in boldface. The predicted amino acid sequence was in the shaded box. Exons were shown in capital letters and introns in small letters. The poly (A) signal was in the box, the poly (A) tail was underlined at the end of sequence.

encoding 38 amino acids from the N-terminus of histone H2A was selected as a potential histone-derived AMP for further study and this peptide was named as Sphistin. The predicted molecular mass of Sphistin was 3.94 kDa and estimated isoelectric point is 12.02.

Helical wheel modeling was employed to show a spatial segregation of hydrophobic and hydrophilic residues (Fig. 5A). The 3D structure of Sphistin was build using modeling tools at SWISS-MODEL website, and PDB 1eqz.1.G was used as a template. Two α-helices were identified in the peptide, among which α1-helix comprised amino acids from Arg^{20} to Arg^{23}, and the α2-helix comprised amino acids from Val^{30} to Leu^{37}. And the electrostatic potential was presented by the blue, white and red surface. As the picture shown Sphistin has got a larger sphere of positive charge net compared to the negative charge net (Fig. 5B).

BLASTP analysis indicated Sphistin showed the highest amino acid identity (85%) to scallop histone H2A-derived AMP and abhisin. Furthermore, it showed 72% and 69% identity to hipposin and buforin I, respectively. And due to the presence of incompleted CDS cloning of histone H2A-derived AMP, the amino acid sequences of published N-terminal domain of histone H2A-derived AMP were used for the phylogenetic analysis (data not shown). In this analysis, all the published histone-derived AMPs from different species were clustered in H2A1, H2A2 or H2A.X group. However, Sphistin branched in a unique subfamily together with H2A.Z.

3.4. Antimicrobial activity of the synthetic Sphistin

The antimicrobial spectrum of the synthetic Sphistin was examined by the method of MIC and MBC assays. As shown in Table 2, synthetic Sphistin exhibited a broad spectrum of inhibitory and bactericidal effect. Notably, Sphistin was effectively against the growth of G^+ bacteria (*S. aureus*, *C. glutamicum*, *Bacillus subtilis*, *Micrococcus lysodeikticus*, *Micrococcus luteus*) and G^- bacteria (*Shigella flexneri*, *Pseudomonas stutzeri*, *Pseudomonas fluorescens*) with an MIC value lower than 1.5 μM, as well as a low bactericidal concentration (MBC<12 μM). In addition, synthetic Sphistin exhibited strong activity against *Aeromonas hydrophila* (MIC 1.5–3 μM), which caused serious diseases in aquiculture farming.

Besides, the bactericidal kinetic effect of Sphistin on *C. glutamicum*, *S. aureus* and *E. coli* MC1061 was evaluated (Fig. 6). Nearly 90% *S. aureus* were killed within 10 min of incubation with 3 μM Sphistin. Approximately 100% killing of *S. aureus* was achieved in 30 min. On the other hand, Sphistin showed more gentler and slower bactericidal activity against *C. glutamicum* and *E. coli* MC1061 than *S. aureus* over the time course. Sphistin (1.5 μM) killed over 90% of *C. glutamicum* and *E. coli* MC1061 within 3 h. And nearly 100% killing of *E. coli* MC1061 was achieved at 5 h.

3.5. Morphological changes of bacteria after incubation with Sphistin

The morphological changes of the *S. aureus*, *E. coli* MC1061 or *P. pastoris* GS115 cells were observed through SEM to understand the mode of action of Sphistin. *S. aureus*, *E. coli* MC1061 or *P. pastoris* GS115 suspensions were treated with Sphistin at the final concentrations of 15 μM, 120 μM or 120 μM respectively. Morphological observations of bacteria treated with Sphistin are presented in Fig. 7. Control bacteria had intact and smooth surface without cell lysis or debris. However, after treatment with Sphistin, the bacterial morphology changed significantly. Cell disrupted and a high degree of cell lysis were especially observed in *S. aureus*. *E. coli* displayed obviously coarse surfaces and debris after treatment. And leakage of cytoplasmic contents were observed in *P. pastoris*.
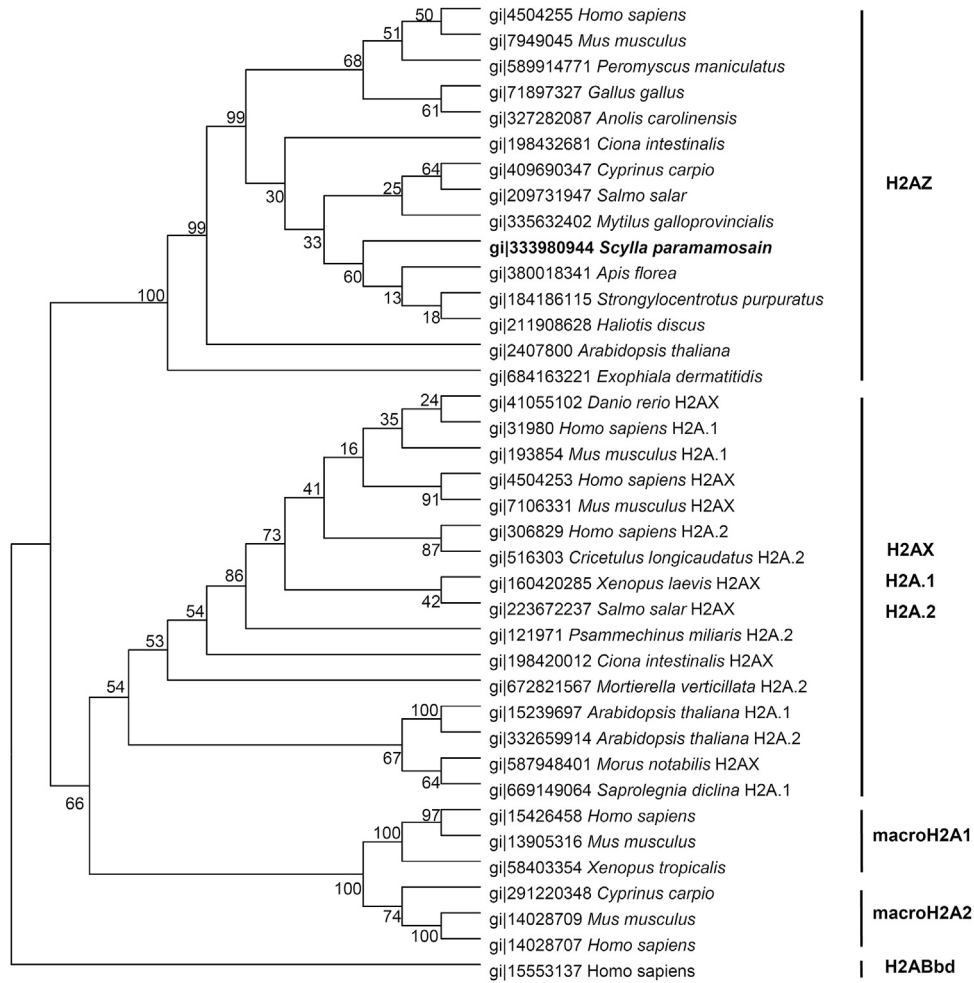
Fig. 2. Phylogenetic analysis of mud crab histone H2A with other histones was constructed by Neighbor-Joining Method using MEGA5 after aligning the amino acid sequences using ClustalW program. The numbers shown at the branches denoted the bootstrap majority consensus values of 1000 replicates. The number before the latin name was GenBank accession numbers.
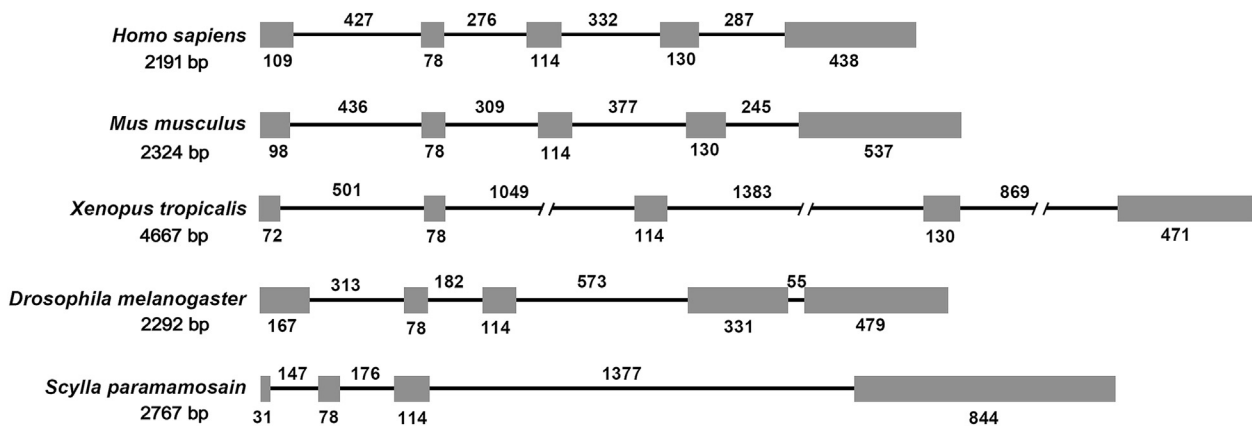

Fig. 3. Comparison of the gene organization of Histone H2A from mud crab with Histone H2A.Z sequences from other organisms. Exons and introns were represented respectively by the gray boxes and black lines. Numbers below and above the boxes respectively indicated exon sizes and intron sizes. The length of exons and introns was drawn to scale except for intron sizes exceeding 800 bp that were indicated with//.

3.6. Sphistin causes adsorption and permeabilization of cell membrane

Cecropin P1, which is a well-known membrane active antimicrobial peptide [38,46,47], was served as a positive control in the study. Addition of 1 μM cecropin P1 to the *E. coli* MC1061 resulted in the membrane permeabilization and luciferase flux which was characterized by a strong peak of light emission. In
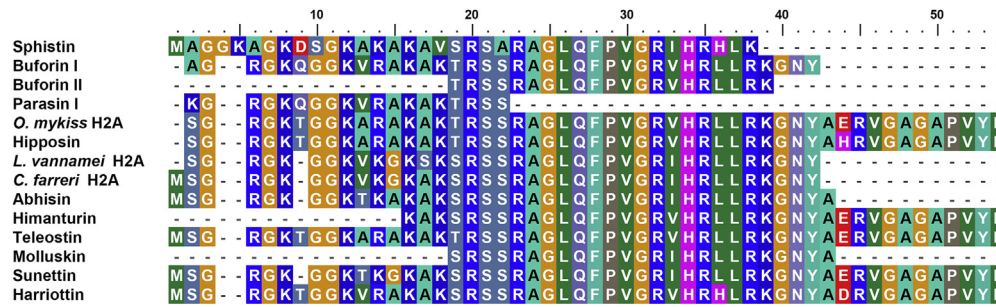
Peptide	Source	Functional Reasearch Method	Position	No. of a.a.	Year	Ref.
Sphistin	*Scylla Paramemosain*	Synthesis	N (1-38)	38	2012	-
Buforin Ⅰ	*Bufo gargarizans*	Purification	N (2-40)	39	1996	[13]
Buforin Ⅱ	*Bufo gargarizans*	Synthesis	N (17-37)	21	1996	[13]
Parasin Ⅰ	*Parasilurus asotus*	Purification	N	19	1998	[19]
O. mykiss H2A 2-52	*Oncorhynchus mykiss*	Purification	N (2-52)	51	2002	[17]
Hipposin	*Hippoglossus hippoglossus L.*	Purification	N (2-52)	51	2003	[18]
L. vannamei H2A 2-39	*Litopenaeus vannamei*	Synthesis/Purification	N (2-39)	38	2004	[23]
C. farreri H2A 1-39	*Chlamys farreri*	Recombinant	N (1-39)	39	2007	[21]
Abhisin	*Haliotis discus discus*	Synthesis	N (1-40)	40	2009	[22]
Himanturin	*Himantura pastinacoides*	-	N	39	2012	[57]
Teleostin	*Tachysurus jella; Cynoglossus semifasciatus*	-	N (1-52)	52	2012	[76]
Molluskin	*Crassostrea madrasensis; Saccostrea Cucullata; Meretrix casta; Ficus gracilis; Bullia vittata*	-	N	25	2012	[77]
Sunettin	*Sunetta scripta*	-	N (1-51)	51	2012	[78]
Harriottin	*Neoharriotta pinnata*	-	N (1-52)	52	2013	[79]

Fig. 4. ClustalW multiple alignment of Sphistin with histone H2A derived AMP, including Buforin I&II, Parasin I, *O. mykiss* H2A, Hipposin, *L. vannamei* H2A, *C. farreri* H2A, Abhisin, Himanturin, Teleostin, Molluskin, Sunettin and Harriottin. The details of these antimicrobial peptide were shown in the table below.

contrast, absence of such a distinct peak after addition of water and Argireline (25 μM), which serve as negative controls, indicates an intact plasma membrane. The result showed that more significant increase of light emission was observed after addition of 50 μM Sphistin in comparison to the cecropin P1. Meanwhile, 25 μM Sphistin also leaded to a light emission peak of *E. coli* MC1061 at 50 s after addition. The results indicated that Sphistin affected bacterium by disruption of its membrane integrity in the same way as cecropin P1 (Fig. 8).

To examine the localization site of Sphistin in microbe, the distribution of Sphistin in microbe was investigated (Fig. 9). The confocal microscopy imaging of bacteria indicated that the action site of Sphistin was at the cell membrame. We did not observed the

internalization of Sphistin in the microbe which implied that Sphistin may not binding to the DNA even when treated by Triton X-100. In the samples without Sphistin, no signal has been detected. The results indicated that Sphistin could bind to the bacterial membrane and enhanced the membrane permeability but did not penetrate it.

3.7. Sphistin binds to bacteria LPS and LTA

The first step in the antimicrobial process is the electrostatic interaction between the positive charges of the antimicrobial peptide and the negatively charged molecules located on the surface of the bacterial cell wall. The LPS binding activity of C-terminal
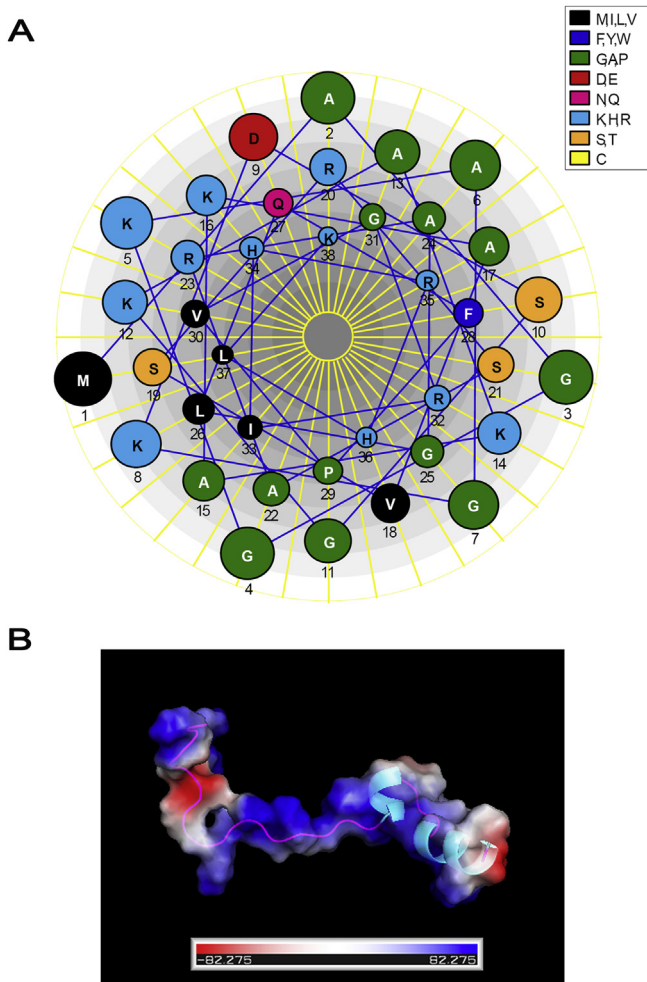
A

B

Fig. 5. Predicted secondary structure and 3D structure of Sphistin. A: Helical wheel diagram showing probable amphiphilic surface of α-helical. B: Three-dimensional structural analysis of Sphistin were build by reference to model PDB 1eqz.1.G at SWISS-MODEL website. The picture were created using the software PyMol. Two α-helical were represented by cyan band. The electrostatic potential was predected, and the positive potentials were shown in blue and negative potentials were in red. (For interpretation of the references to color in this figure legend, the reader is referred to the web version of this article.)

Table 2
Mimimum inhibitory concentration and minimum bactericidal concentration of Sphistin synthetic peptide.

Microorganisms	CGMCC No.[c]	MIC (μM)	MBC (μM)
Gram-positive bacteria			
Micrococcus lysodeikticus Fleming	CGMCC 1.0634	<1.5	<1.5
Micrococcus luteus	CGMCC 1.634	<1.5	1.5[a]–3[b]
Staphylococcus aureus	CGMCC 1.363	<1.5	<3
Bacillus subtilis	CGMCC 1.108	<1.5	<1.5
Corynebacterium glutamicum	CGMCC 1.1886	<1.5	<1.5
Staphylococcus epidermidis	CGMCC 1.2429	6–12	24–48
Bacillus cereus	CGMCC 1.447	>48	NT
Gram-negative bacteria			
Pseudomonas fluorescens	CGMCC 1.0032	<1.5	1.5–3
Shigella flexneri	CGMCC 1.1868	<1.5	6–12
Pseudomonas stutzeri	CGMCC 1.1803	<1.5	<1.5
Aeromonas hydrophila	CGMCC 1.0927	1.5–3	6–12
Escherichia coli	CGMCC 1.2389	1.5–3	>96
Escherichia coli MC1061[e]		3–6	12–24
Pseudomonas aeruginosa	CGMCC 1.0205	24–48	>96
Vibrio parahaemloyticus	CGMCC 1.1615	>48	NT[f]
Vibrio alginolyticus	CGMCC 1.1833	>48	NT
Vibrio harveyi	CGMCC 1.1593	>48	NT
Vibrio fluvialis	CGMCC 1.1609	>48	NT
Yeast			
Pichia pastoris[d]	Invitrogen Biotech	6–12	24–48
Candida albicans	CGMCC 2.2411	>48	NT

[a], [b] MIC is expressed as the interval 'a–b', where 'a' is the highest concentration tested at which microorganisms are growing and 'b' is the lowest concentration that causes 100% visual growth inhibition after 24 h of incubation with bacteria or 48 h of incubation with yeast. MBC represents the lowest concentration at which no microorganism grew on the appropriate plate after incubation with the MIC assay mixture overnight for bacteria and 2 d for yeast.
[c] CGMCC No. indicates China General Microbiological Culture Collection Center number. [d] Strain from Invitrogen Biotech.
[e] *E. coli* MC1061 transferred with luciferase gene vector pCSS962 was provided by Dr. Chun Li.
[f] NT, not tested.

3.9. Immunomodulatory activities of synthetic Sphistin peptide

To further characterize the immunomodulation activity of Sphistin, expression of immune-related mRNA in crab haemolymph after Sphistin treatment for 3, 6, 12 and 24 h were determined. As shown in Fig. 12, the mRNA expression level of TNF receptor super family (TNFRSF), LPS-induced TNF-α factor (LITAF) and Spätzle were significantly upregulated at 6 h post Sphistin incubation. However, the expression of TNF super family (TNFSF) and antimicrobial peptide crustin and ALF2 were unaffected or show weak variation under Sphistin treatment. These results suggested that Sphistin possibly activated and induced an inflammatory response in crab haemolymph.

4. Discussion

Antimicrobial peptides (AMPs) are multi-functional peptides in the innate immune system whose fundamental biological role has been proposed to be focused on the elimination of pathogenic microorganisms [49]. Histone proteins are primarily involved in DNA packaging and regulation of DNA replication and transcription. These proteins form the basic building blocks of chromatin structure when the four core histone proteins, H2A, H2B, H3 and H4 come together as heterodimers to constitute the nucleosome and H1/H5 acts as the linker histones. Until now, a number of histone derived antimicrobial peptides have been identified from both vertebrate and invertebrate. The histone gene in the present study was cloned from the haemolymphs of mud crab *S. paramamosain*, which possessed typical histone signature domain and over 80% amino acid identity to known
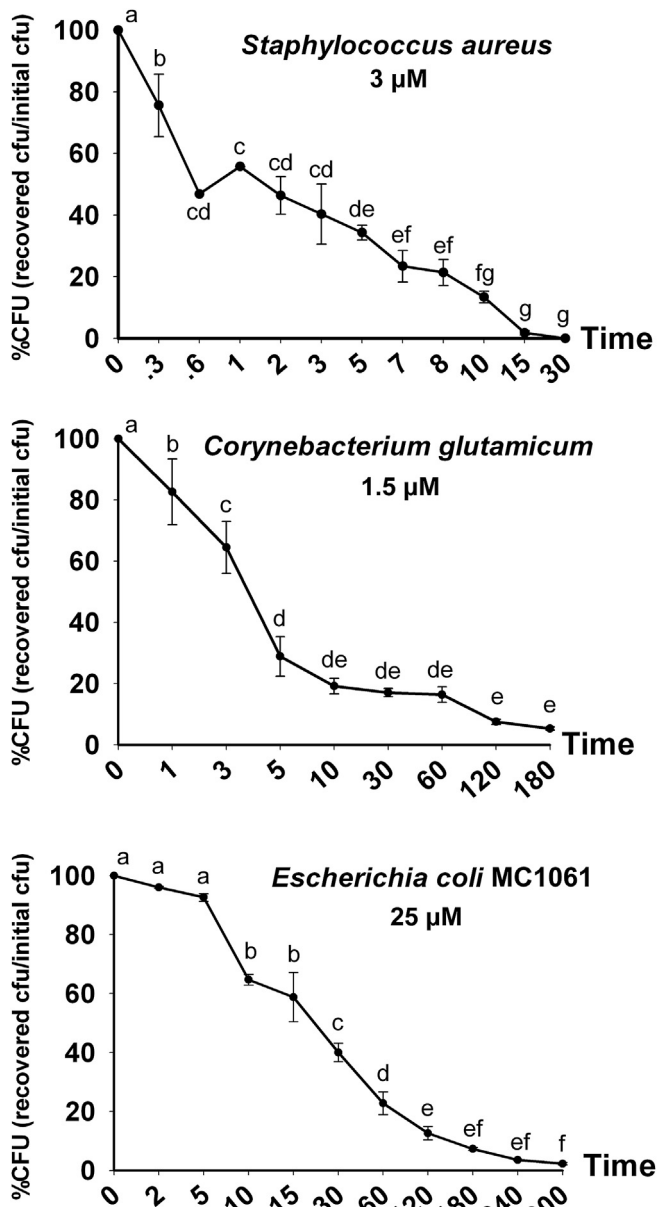
moiety of histones have been reported in previous research [48]. However, Sphistin which is the N-terminus of histone showed membrane binding activity according to the result of confocal microscopy imaging of bacteria. As a result, the binding characters of Sphistin to the cell wall components were examined by ELISA (Fig. 10). It was found that Sphistin binded to LPS and LTA in a concentration dependent manner. Additionally, the apparent constant of dissociation for the binding of the Sphistin to LPS (K_d = 100.3 μM) was higher than LTA (K_d = 55.6 μM). It was indicated that the binding activity of Sphistin towards LTA was stronger than that of LPS.

3.8. Effect of the synthetic Sphistin peptide on cell cytotoxicity

A MTT assay was used to determine whether the Sphistin displayed toxicity towards mouse MC3T3-E1 and crab haemolymph over a wide range of Sphistin concentrations (0–100 μg/mL) in 24 h. Results showed that Sphistin did not result in a decrease of cell viability even at the highest concentration tested (100 μg/mL) (Fig. 11).

Fig. 6. Bactericidal kinetic curves of synthesized Sphistin. The minimal bactericidal concentration against Gram-positive *S. aureus* and *C. glutamicum* and Gram-negative *E. coli* MC1061 was used. Data were represented as the mean ± S.D. (n = 3) bacterial recovery index. The same letters indicated no significant difference between different time points, and different letters indicated statistically significant differences between time points. (P < 0.05, one-way ANOVA followed by the Tukey post hoc test.)

H2A counterparts. According to the phylogenetic tree and BLASTP result, the mud crab histone belonged to H2A.Z sub-family, of which the amino acid sequence was remarkably conserved in comparison with the other vertebrates and invertebrates histone H2A.Z. However the gene structure of the mud crab histone H2A was different from other reported H2A.Z. The genomic DNA organization of the mud crab H2A.Z showed only four exons and three introns other than five exons and four introns in other four species. The diversity in the length and the number of exons and introns may indicate the erratic evolution of histone H2A.Z [50].

Several studies on histone mechanism *in vivo* have demonstrated that histone is activated with the inflammatory stimulation and exerts its activity by releasing in the haemolymphs or some specific tissues with a short processed histone-derived peptide. Park reports that Parasin I, an antimicrobial peptide derived from histone H2A in the catfish is extracellularly secreted to the epithelial mucosal layer and then processed to be potent antimicrobial peptide responding to the tissue damage [19]. Patat indicates in a study on the Pacific white shrimp that the antimicrobial activity of histones is probably dependent on its derived proteins that are isolated from haemolymphs, the circulating immune cells of invertebrates [23]. Not only the histones directly isolated in the haemolymph, but also the histones associated with haemolymph extracellular traps (ETs) possess strong antimicrobial activities against microbes. Histones have been proved to play critical antimicrobial roles in neutrophil extracellular traps (NETs) in higher vertebrates [2,51–53]. ETs act in a similar manner in invertebrates as NETs that entrap and kill microbes by releasing extracellular fibers formed by DNA, histones and cytoplasmic antimicrobial proteins [54–56]. The research on haemolymph ETs in *Crassostrea gigas* provides the evidence that the antimicrobial histone-derived fragment is shown to be associated with extracellular DNA networks released by haemolymphs [55]. Meanwhile, the histone accumulation and hemocyte-infiltrated interstitial tissues consistently existed in the surrounding wounds of *C. gigas* [55]. In addition, our present study also showed that the expression of histone H2A in haemolymphs of the mud crab was up-regulated post microbial challenge. All of the reported data indicated that histones might be a widely conserved and original component of innate immunity in both vertebrates and invertebrates. It would be proposed that the mechanism of histone activation in haemolymphs might refer to up-expression under stimulation, accumulation along with haemolymph-infiltrate wounded tissue, deimination and proteolytic cleavage [52,53,55] to form antimicrobial fragments and release from haemolymph or formation of ETs. However, the clear mechanism of histone activation in mud crab remains further investigation.

The antimicrobial activity of N-terminus of histone H2A has been reported in several species by using the synthetic peptides or purified peptide from different organisms [13,18,22,23]. In the present study, the synthetic N-terminus of histone H2A, Sphistin, exhibited strong antimicrobial activity against various G$^+$ and G$^-$ pathogenic bacteria such as *S. aureus*, *Staphylococcus epidermidis* and *S. flexneri*. Notably, Sphistin was effectively at the concentration lower than 3 µM against the growth of *A. hydrophila*, *P. fluorescens* and *P. stutzeri* which were all important pathogens in aquiculture farming. All these features indicated that the Sphistin, like other N-terminal fragment of histone H2A, was a potential AMP in crabs.

Based on the sequence and structure analysis, it was found that Sphistin was a amphipathic and α-helix rich cationic antimicrobial peptide and similar to other know histones derived AMPs [21,22,57,58]. The antimicrobial mode of α-helical cationic peptides has been proposed to occur via three general mechanisms: (i) binding to the cell surface (ii) membrane permeabilization and (iii) secondary effects (DNA/protein binding, membrane compositional rearrangements, interference with essential cellular machinery, etc.) [59–61]. Previous studies reveal that the antimicrobial mechanism of histone derived AMPs involve not only membrane disruption but also secondary effects such as interactions with nucleic acids [57,62,63], and the mechanism is discrepancy among different source peptides due to the position and length of the histone derived peptide. Our findings on the Sphistin study testified the previous results.

It is reported that the electrostatic interaction between the positively charged peptides and the negatively charged moieties on the bacterial membrane plays important roles in the antimicrobial process of AMPs [64,65]. Sphistin was predicted to be a
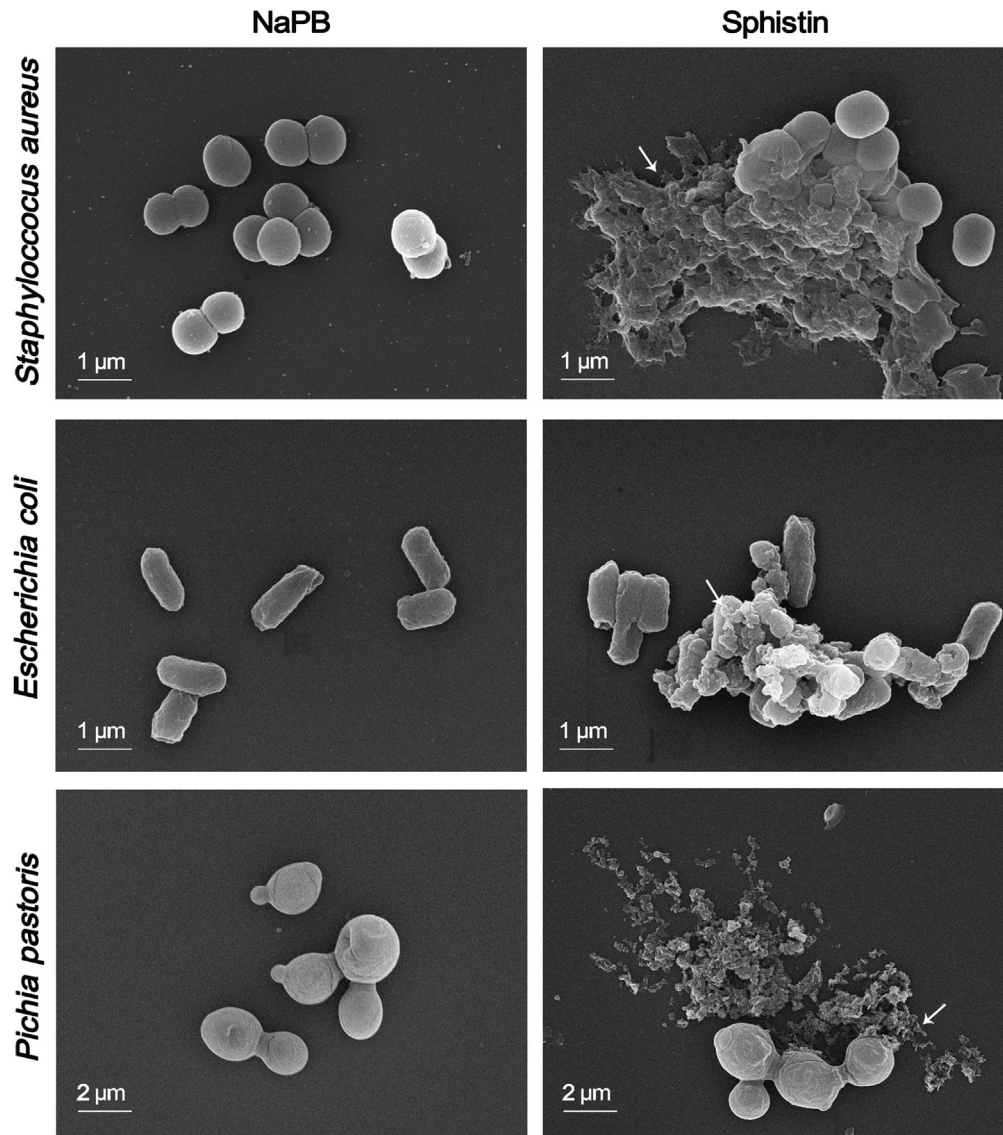
Fig. 7. Morphological observations of *S. aureus*, *E. coli* MC1061 or *P. pastoris* GS115 by scanning electron microscopy. Microbe were treated with NaPB (left column, control) and synthetic Sphistin (right colunm), respectively. White arrows indicated coarse surfaces, cellular debris and cell lysis, respectively.

cationic antimicrobial peptide, with the positive charge of +9. The 3D structure picture indicated that Sphistin displayed a large positive electrostatic surface. The cationic characteristic of Sphistin made it possible to exert its antimicrobial function via electrostatic attraction. Our research also provided evidence that Sphistin was capable of binding to LPS and LTA in dose-dependent manner, which belonged to the Gram-negative and Gram-positive bacteria cell wall component, respectively. Sphistin clearly exhibited binding affinity to LPS and LTA at as low as 10 μg/mL. Based on our results, it would be speculated that the initial step in the antimicrobial mechanism of Sphistin probably involved electrostatical attraction to negatively charged microbial surfaces. Moreover, histone is also reported to possess LPS binding activity as a pattern recognition receptor [66] or an endotoxin-neutralizing peptide [3,4], however the high binding activity to the LPS is mostly related to either the whole histone or the C-terminal of the histone 2A-derived AMP [48]. Therefore, it is the first time to report that the N-terminal of histone 2A-

derived AMP from marine crabs possessed LPS and LTA binding activity. Besides, the opposite position of hydrophobic and hydrophilic residues in the secondary structure prediction indicated a good amphiphilic characteristic of Sphistin. As an amphiphilic α-helical antimicrobial peptide, Sphistin might attach to the bacterial cell surface by making their axes parallel to the membrane surface, with the hydrophobic partitioning interacting strongly with phospholipid bilayers. Whereas the insertion of the peptide and disruption of the membrane integrity could subsequently occur by various mechanisms [61].

The membrane permeabilizing mechanism of antimicrobial activities has been proved in many AMPs, as studied for magainin 2, melittin and cecropin [47]. In our study, it was observed under a confocal laser-scanning microscope that Sphistin was located on the membrane of microbe without translocating internally to the cell. In addition, a real-time membrane integrity assay further verfied the increase of membrane permeability and the SEM investigation demonstrated the damage of cell surface and
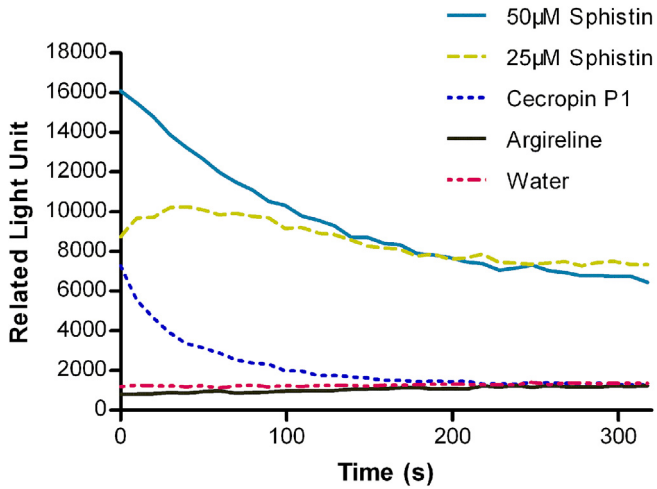
Fig. 8. Effect of Sphistin on bacterial membrane integrity. Light emission kinetics of *E. coli* MC1061 cells treated with Sphistin (25 μM/50 μM) or one of the controls at t = 0 is plotted as a function of time for 5 min starting 20 s after peptide addition. The lag time is due to plate handling and shaking inside the multi-plate-reader and is therefore excluded from the graph. The light peak after cecropin P1 addition (1 μM, dotted line) was the result of membrane permeabilization due to activity of the membraneactive control peptide cecropin P1. The same current appeared after addition of 50 μM Sphistin (blue solid line) and 25 μM Sphistin (dashed line). Water (dash-dotted line) and Argireline (25 μM, black solid line) serve as controls, indicated an intact plasma membrane. (For interpretation of the references to color in this figure legend, the reader is referred to the web version of this article.)
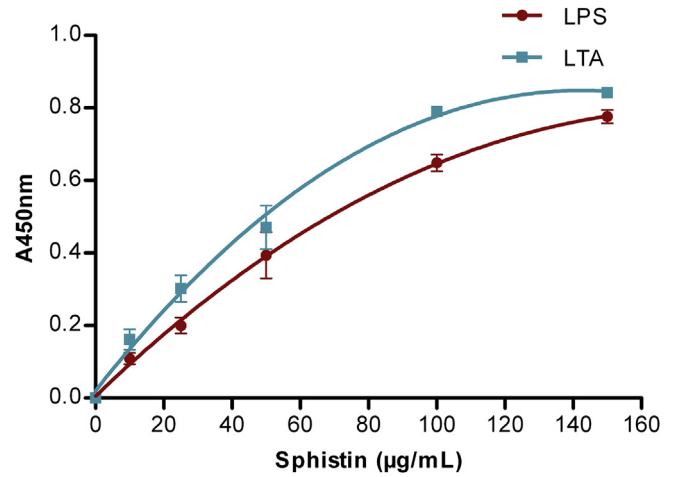
Fig. 10. Analysis of the binding affinity between Sphistin protein and the bacterial associated molecules. The binding affinity of Sphistin to LPS and LTA was tested by ELISA. Absorbance of each well was measured at 450 nm. Circular: lipopolysaccharide, LPS; Square: Lipoteichoic acid, LTA.

leakage of cytoplasmic contents. All of the results provided the strong evidence that Sphistin exerted antimicrobial activity via adsorption, subsequently permeabilization and finally destruction of bacterial cell membranes but not penetrating it. These observations are consistent with the membrane permeabilizing mechanism observed in the previous studies of Hip AB domain of hipposin, which is analogous to Sphistin activity. As reported that
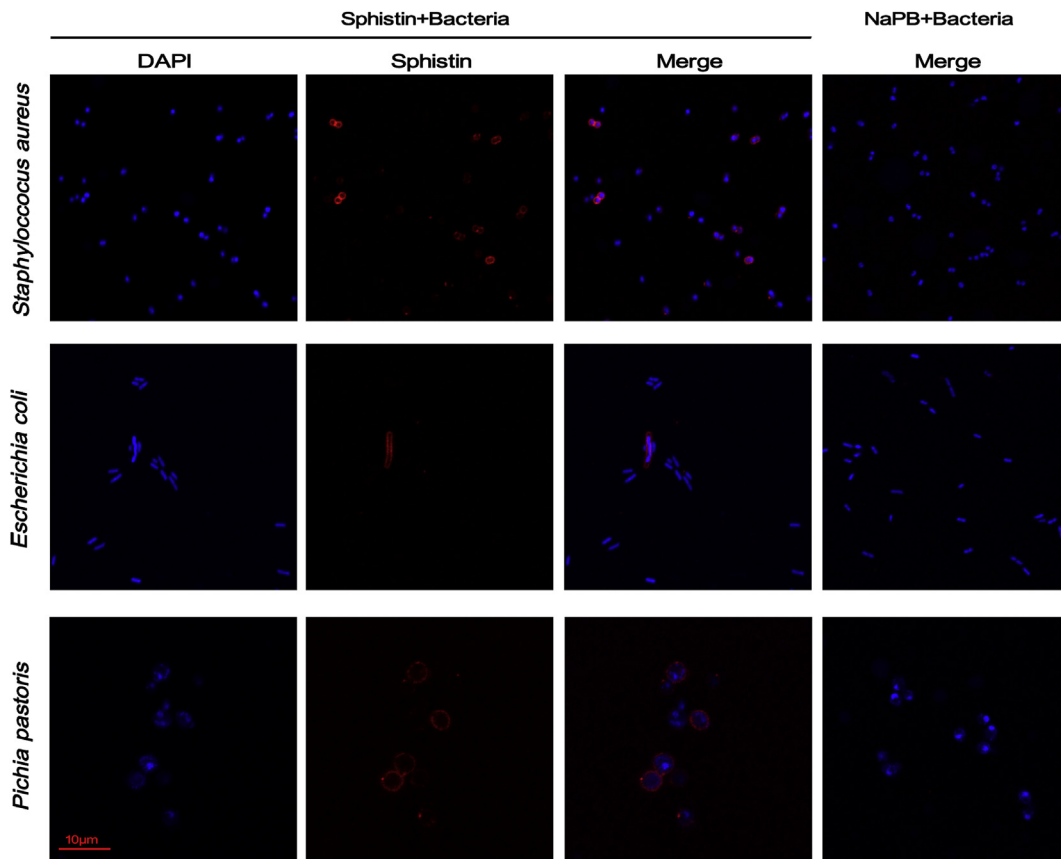
Fig. 9. Localization of Sphistin in *S. aureus*, *E. coli* MC1061 and *P. pastoris* cells by confocal laser scanning microscopy. Cells were treated and untreated with Sphistin. For each treatment, fluorescence of DAPI or Sphisitin images, as well as merged images, were presented. For the untreated cell, only merge images were shown.
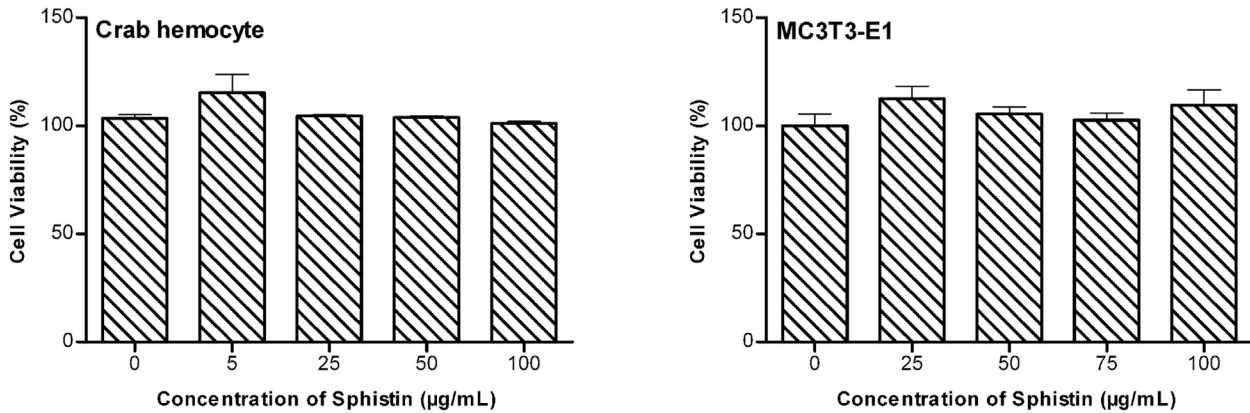
Fig. 11. Effects of Sphistin on cell viability of mouse MC3T3-E1 and crab haemolymph. Cell were incubated with synthetic Sphistin peptide (0–100 μg/mL) at 37 °C and 20 °C for 24 h, respectively. Cell viability was determined by cell proliferation assay and represented as percentage respective to the control. (P < 0.05, one way ANOVA followed by Tukey post hoc test.)
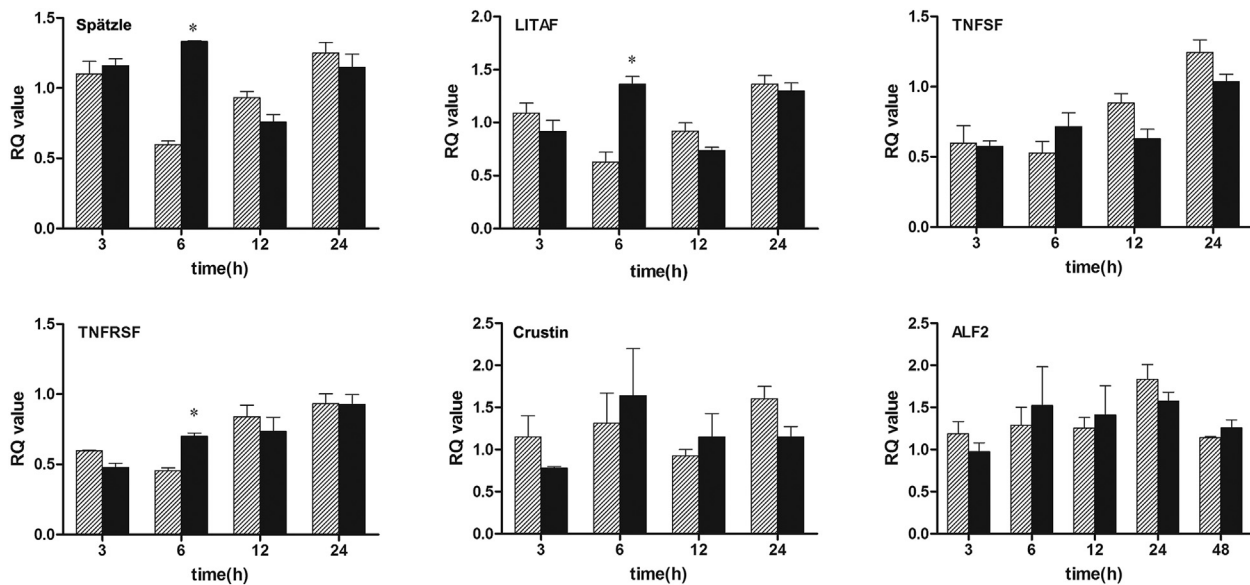

Fig. 12. Quantification of transcript levels by relative qPCR. RNA from crab haemolymph was cotreated with 25 μg/ml Sphistin (black). The group not treated with the peptide served as the control (gray). Samples were collected after treatment for 3, 6, 12 and 24 h. Transcript abundance was normalized to β-actin expression. Each bar represents the mean value from four determinations with the standard error. Data with "*" significantly differed (p < 0.05) between treatment and control.

both of parasin I(19aa) [62] and HipA domain (1-15aa) of hipposin [63] are mainly responsible for the membrane-permeabilizing activity, the presence of the N-terminal of Sphistin may play an important role in the membrane permeabilization during anti-microbial process. Furthermore, Koo et al. suggests that the α-helical structure of parasin I is necessary for the membrane localization [62]. However, the first α-helical position of Sphistin predicted by 3D protein structure analysis was quite different from that of parasin I, and thus the correlation between membrane permeabilizing mechanism and α-helix in Sphistin requires more further research.

Besides the antimicrobial activity, AMPs are reported to have a variety of immunomodulational activities, including endotoxin neutralization, pro- and anti-apoptotic effects, chemoattraction, wound repair, angiogenesis, tumour surveillance, and enhancement of the production of cytokines and chemokines [67]. Many antimicrobial peptides could induce the expression of various pro-inflammatory cytokines and chemokine, for example human cationic antibacterial protein LL37, rat antibacterial cathelicidin

rCRAMP and insect antimicrobial peptide cecropin B [68–70]. However, less attention has been given to the immunomodulational activity of histone except for Atlantic cod histone which is reported to activate macrophage through inducing production of superoxide [5]. In our present study, the potential immunomodulational activity of the mud crab histone was for the first time explored. The synthetic Sphistin could significantly upregulate the mRNA expression of Spätzle, LITAF, and TNFRSF and the TNFSF weakly increased at 6 h. As it is known, LITAF is a transcription factor involved in the pathway linking LPS/TLR/MyD88/LITAF to TNF [71] and Spätzle is an extracellular ligand of Toll which realizes the activation of the Toll pathway in invertebrate [72,73]. Therefore, Sphistin might enhance the TNF expression though Toll-LITAF pathway and also activate the TNF-TNFR system, by which it would be derived for the first time that the mud crab Sphistin might play a role in innate immunity through the activation of haemolymphs to generate the proinflammatory cytokine.

The potential cytotoxicity to the host cells is one of the limitations that restricts the development and application of

antimicrobial peptides in aquaculture and veterinary medicine. However, there is not any report on the histone derived peptides which have exhibited cytotoxic activity against normal eukaryotic cells. The toad histone H2A-derived peptide buforin IIb is cytotoxic to cancer cells but not effect on normal eukaryotic cells [74]. Synthetic abhisin shows cytotoxic effects by reducing cell viability in leukemia cancer (THP-1) cells but not in normal fibroblast vero cells [22]. Similarly, the histones purified from chicken erythrocytes do not display toxicity towards mammalian cells through a hemolytic assay [75]. In the study, Sphistin did not show any effect on the viability of crab and mammal cells even at the highest concentration tested (100 μg/mL). Thus, Sphistin could become a potential antimicrobial agent for aquaculture and veterinary medicine due to its potent antimicrobial activity and less cytotoxicity.

In summary, the N-terminus of mud crab H2A designated as Sphistin, was a new potential AMP and had the main characteristic features with net positive charges and higher hydrophobic residues. Sphistin showed antimicrobial activity against pathogenic bacteria and yeast and its antimicrobial mechanism was likely by the way of adsorption and subsequently permeabilization of the cell membrane but not penetrating the cell membrane. Moreover, Sphistin (100 μg/mL) did not display toxicity towards either mammal or crab normal cells. The ability of Sphistin inducing the expression of some immune-associated genes indicated a potential immunoregulation role through the activation of haemolymphs. Totally, Sphistin appeared to be a good candidate for future application in aquaculture farming, therapeutics or host defense modulation in invertebrates.

Acknowledgments

References

[1] B.D. Strahl, C.D. Allis, The language of covalent histone modifications, Nature 403 (2000) 41–45.

[2] M.H. Parseghian, K.A. Luhrs, Beyond the walls of the nucleus: the role of histones in cellular signaling and innate immunity, Biochem. Cell Biol. 84 (2006) 589–604.

[3] H.S. Kim, J.H. Cho, H.W. Park, H. Yoon, M.S. Kim, S.C. Kim, Endotoxin-neutralizing antimicrobial proteins of the human placenta, J. Immunol. 168 (2002) 2356–2364.

[4] S.S. Witkin, I.M. Linhares, A.M. Bongiovanni, C. Herway, D. Skupski, Unique alterations in infection-induced immune activation during pregnancy, BJOG Int. J. Obstet. Gynaecol. 118 (2011) 145–153.

[5] G.M. Pedersen, A. Gildberg, K. Steiro, R.L. Olsen, Histone-like proteins from Atlantic cod milt: stimulatory effect on Atlantic salmon leucocytes *in vivo* and *in vitro*, Comp. Biochem. Physiol. Part B Biochem. Mol. Biol. 134 (2003) 407–416.

[6] R. Reichhart, M. Zeppezauer, H. Jornvall, Preparations of homeostatic thymus hormone consist predominantly of histones 2A and 2B and suggest additional histone functions, Proc. Natl. Acad. Sci. U. S. A. 82 (1985) 4871–4875.

[7] A. Konishi, S. Shimizu, J. Hirota, T. Takao, Y. Fan, Y. Matsuoka, et al., Involvement of histone H1.2 in apoptosis induced by DNA double-strand breaks, Cell 114 (2003) 673–688.

[8] F. Jacobsen, A. Baraniskin, J. Mertens, D. Mittler, A. Mohammadi-Tabrisi, S. Schubert, et al., Activity of histone H1.2 in infected burn wounds, J. Antimicrob. Chemother. 55 (2005) 735–741.

[9] S.J. Howell, D. Wilk, S.P. Yadav, C.L. Bevins, Antimicrobial polypeptides of the human colonic epithelium, Peptides 24 (2003) 1763–1770.

[10] F.R. Rose, K. Bailey, J.W. Keyte, W.C. Chan, D. Greenwood, Y.R. Mahida, Potential role of epithelial cell-derived histone H1 proteins in innate antimicrobial defense in the human gastrointestinal tract, Infect. Immun. 66 (1998) 3255–3263.

[11] T. Drab, J. Kracmerova, E. Hanzlikova, T. Cerna, R. Litvakova, A. Pohlova, et al., The antimicrobial action of histones in the reproductive tract of cow, Biochem. Biophys. Res. Commun. 443 (2014) 987–990.

[12] U. Silphaduang, M.T. Hincke, Y. Nys, Y. Mine, Antimicrobial proteins in chicken reproductive system, Biochem. Biophys. Res. Commun. 340 (2006) 648–655.

[13] C.B. Park, M.S. Kim, S.C. Kim, A novel antimicrobial peptide from *Bufo bufo gargarizans*, Biochem. Biophys. Res. Commun. 218 (1996) 408–413.

[14] G. Bergsson, B. Agerberth, H. Jornvall, G.H. Gudmundsson, Isolation and identification of antimicrobial components from the epidermal mucus of Atlantic cod (*Gadus morhua*), FEBS J. 272 (2005) 4960–4969.

[15] D. Robinette, S. Wada, T. Arroll, M.G. Levy, W.L. Miller, E.J. Noga, Antimicrobial activity in the skin of the channel catfish *Ictalurus punctatus*: characterization of broad-spectrum histone-like antimicrobial proteins, Cell. Mol. life Sci. CMLS 54 (1998) 467–475.

[16] R.C. Richards, D.B. O'Neil, P. Thibault, K.V. Ewart, Histone H1: an antimicrobial protein of Atlantic salmon (*Salmo salar*), Biochem. Biophys. Res. Commun. 284 (2001) 549–555.

[17] J.M. Fernandes, G.D. Kemp, M.G. Molle, V.J. Smith, Anti-microbial properties of histone H2A from skin secretions of rainbow trout, *Oncorhynchus mykiss*, Biochem. J. 368 (2002) 611–620.

[18] G.A. Birkemo, T. Luders, O. Andersen, I.F. Nes, J. Nissen-Meyer, Hipposin, a histone-derived antimicrobial peptide in Atlantic halibut (*Hippoglossus hippoglossus L.*), Biochim. Biophys. Acta 1646 (2003) 207–215.

[19] I.Y. Park, C.B. Park, M.S. Kim, S.C. Kim, I. Parasin, an antimicrobial peptide derived from histone H2A in the catfish, *Parasilurus asotus*, FEBS Lett. 437 (1998) 258–262.

[20] J.M. Fernandes, G. Molle, G.D. Kemp, V.J. Smith, Isolation and characterisation of oncorhyncin II, a histone H1-derived antimicrobial peptide from skin secretions of rainbow trout, *Oncorhynchus mykiss*, Dev. Comp. Immunol. 28 (2004) 127–138.

[21] C. Li, L. Song, J. Zhao, L. Zhu, H. Zou, H. Zhang, et al., Preliminary study on a potential antibacterial peptide derived from histone H2A in hemocytes of scallop *Chlamys farreri*, Fish Shellfish Immunol. 22 (2007) 663–672.

[22] M. De Zoysa, C. Nikapitiya, I. Whang, J.S. Lee, J. Lee, Abhisin: a potential antimicrobial peptide derived from histone H2A of disk abalone (*Haliotis discus discus*), Fish Shellfish Immunol. 27 (2009) 639–646.

[23] S.A. Patat, R.B. Carnegie, C. Kingsbury, P.S. Gross, R. Chapman, K.L. Schey, Antimicrobial activity of histones from hemocytes of the Pacific white shrimp, Eur. J. Biochem. FEBS 271 (2004) 4825–4833.

[24] M.K. Chaurasia, R. Palanisamy, P. Bhatt, V. Kumaresan, A.J. Gnanam, M. Pasupuleti, et al., A prawn core histone 4: derivation of N- and C-terminal peptides and their antimicrobial properties, molecular characterization and mRNA transcription, Microbiol. Res. 170 (2015) 78–86.

[25] J. Arockiaraj, A.J. Gnanam, V. Kumaresan, R. Palanisamy, P. Bhatt, M.K. Thirumalai, et al., An unconventional antimicrobial protein histone from freshwater prawn *Macrobrachium rosenbergii*: analysis of immune properties, Fish Shellfish Immunol. 35 (2013) 1511–1522.

[26] H.S. Kim, H. Yoon, I. Minn, C.B. Park, W.T. Lee, M. Zasloff, et al., Pepsin-mediated processing of the cytoplasmic histone H2A to strong antimicrobial peptide buforin I, J. Immunol. 165 (2000) 3268–3274.

[27] J.H. Cho, I.Y. Park, H.S. Kim, W.T. Lee, M.S. Kim, S.C. Kim, Cathepsin D produces antimicrobial peptide parasin I from histone H2A in the skin mucosa of fish, FASEB J. Off. Publ. Fed. Am. Soc. Exp. Biol. 16 (2002) 429–431.

[28] D. Schnapp, G.D. Kemp, V.J. Smith, Purification and characterization of a proline-rich antibacterial peptide, with sequence similarity to bactenecin-7, from the haemocytes of the shore crab, *Carcinus maenas*, Eur. J. Biochem. FEBS 240 (1996) 532–539.

[29] L. Khoo, D.W. Robinette, E.J. Noga, Callinectin, an Antibacterial Peptide from Blue Crab, *Callinectes sapidus*, Hemocytes, Mar. Biotechnol. 1 (1999) 44–51.

[30] K.J. Wang, W.S. Huang, M. Yang, H.Y. Chen, J. Bo, S.J. Li, et al., A male-specific expression gene, encodes a novel anionic antimicrobial peptide, scygonadin, in *Scylla serrata*, Mol. Immunol. 44 (2007) 1961–1968.

[31] C. Imjongjirak, P. Amparyup, A. Tassanakajon, S. Sittipraneed, Anti-lipopolysaccharide factor (ALF) of mud crab *Scylla paramamosain*: molecular cloning, genomic organization and the antimicrobial activity of its synthetic LPS binding domain, Mol. Immunol. 44 (2007) 3195–3203.

[32] S.V. Sperstad, T. Haug, T. Vasskog, K. Stensvag, Hyastatin, a glycine-rich multi-domain antimicrobial peptide isolated from the spider crab (*Hyas araneus*) hemocytes, Mol. Immunol. 46 (2009) 2604–2612.

[33] K. Stensvag, T. Haug, S.V. Sperstad, O. Rekdal, B. Indrevoll, O.B. Styrvold, Arasin 1, a proline-arginine-rich antimicrobial peptide isolated from the spider crab, Hyas araneus, Dev. Comp. Immunol. 32 (2008) 275–285.

[34] C. Imjongjirak, P. Amparyup, A. Tassanakajon, Two novel antimicrobial peptides, arasin-likeSp and GRPSp, from the mud crab *Scylla paramamosain*, exhibit the activity against some crustacean pathogenic bacteria, Fish Shellfish Immunol. 30 (2011) 706–712.

[35] F.Y. Chen, H.P. Liu, J. Bo, H.L. Ren, K.J. Wang, Identification of genes differentially expressed in hemocytes of *Scylla paramamosain* in response to lipopolysaccharide, Fish Shellfish Immunol. 28 (2010) 167–177.

[36] P. Bulet, J.L. Dimarcq, C. Hetru, M. Lagueux, M. Charlet, G. Hegy, et al., A novel inducible antibacterial peptide of Drosophila carries an O-glycosylated substitution, J. Biol. Chem. 268 (1993) 14893–14897.

[37] S.B. Tencza, J.P. Douglass, D.J. Creighton Jr., R.C. Montelaro, T.A. Mietzner,

Novel antimicrobial peptides derived from human immunodeficiency virus type 1 and other lentivirus transmembrane proteins, Antimicrob. Agents Chemother. 41 (1997) 2394–2398.

[38] L. Cai, J.J. Cai, H.P. Liu, D.Q. Fan, H. Peng, K.J. Wang, Recombinant medaka (*Oryzias melastigmus*) pro-hepcidin: multifunctional characterization, Comp. Biochem. Physiol. Part B Biochem. Mol. Biol. 161 (2012) 140–147.

[39] C. Li, H.M. Blencke, L.C. Smith, M.T. Karp, K. Stensvag, Two recombinant peptides, SpStrongylocins 1 and 2, from Strongylocentrotus purpuratus, show antimicrobial activity against Gram-positive and Gram-negative bacteria, Dev. Comp. Immunol. 34 (2010) 286–292.

[40] M. Virta, K.E. Akerman, P. Saviranta, C. Oker-Blom, M.T. Karp, Real-time measurement of cell permeabilization with low-molecular-weight membranolytic agents, J. Antimicrob. Chemother. 36 (1995) 303–315.

[41] M. Gonzalez, B. Romestand, J. Fievet, A. Huvet, M.C. Lebart, Y. Gueguen, et al., Evidence in oyster of a plasma extracellular superoxide dismutase which binds LPS, Biochem. Biophys. Res. Commun. 338 (2005) 1089–1097.

[42] Q.X. Zhang, H.P. Liu, R.Y. Chen, K.L. Shen, K.J. Wang, Identification of a serine proteinase homolog (Sp-SPH) involved in immune defense in the mud crab Scylla paramamosain, PloS One 8 (2013) e63787.

[43] J. Ding, F.Y. Chen, S.Y. Ren, K. Qiao, B. Chen, K.J. Wang, Molecular characterization and promoter analysis of crustacean heat shock protein 10 in *Scylla paramemosain*, Genome Natl. Res. Counc. Can. 56 (2013) 273–281.

[44] C. Redon, D. Pilch, E. Rogakou, O. Sedelnikova, K. Newrock, W. Bonner, Histone H2A variants H2AX and H2AZ, Curr. Opin. Genet. Dev. 12 (2002) 162–169.

[45] C.M. Weber, S. Henikoff, Histone variants: dynamic punctuation in transcription, Genes Dev. 28 (2014) 672–682.

[46] T.D. Lockey, D.D. Ourth, Formation of pores in *Escherichia coli* cell membranes by a cecropin isolated from hemolymph of *Heliothis virescens* larvae, Eur. J. Biochem. FEBS 236 (1996) 263–271.

[47] K.A. Brogden, Antimicrobial peptides: pore formers or metabolic inhibitors in bacteria? Nat. Rev. Microbiol. 3 (2005) 238–250.

[48] L.A. Augusto, P. Decottignies, M. Synguelakis, M. Nicaise, P. Le Marechal, R. Chaby, Histones: a novel class of lipopolysaccharide-binding molecules, Biochemistry 42 (2003) 3929–3938.

[49] G. Diamond, N. Beckloff, A. Weinberg, K.O. Kisich, The roles of antimicrobial peptides in innate host defense, Curr. Pharm. Des. 15 (2009) 2377–2392.

[50] Y. Bao, L. Li, F. Xu, G. Zhang, Intracellular copper/zinc superoxide dismutase from bay scallop Argopecten irradians: its gene structure, mRNA expression and recombinant protein, Fish Shellfish Immunol. 27 (2009) 210–220.

[51] V. Brinkmann, U. Reichard, C. Goosmann, B. Fauler, Y. Uhlemann, D.S. Weiss, et al., Neutrophil extracellular traps kill bacteria, Science 303 (2004) 1532–1535.

[52] M.J. Kaplan, M. Radic, Neutrophil extracellular traps: double-edged swords of innate immunity, J. Immunol. 189 (2012) 2689–2695.

[53] V. Brinkmann, A. Zychlinsky, Beneficial suicide: why neutrophils die to make NETs, Nat. Rev. Microbiol. 5 (2007) 577–582.

[54] T.H. Ng, S.H. Chang, M.H. Wu, H.C. Wang, Shrimp hemocytes release extracellular traps that kill bacteria, Dev. Comp. Immunol. 41 (2013) 644–651.

[55] A.C. Poirier, P. Schmitt, R.D. Rosa, A.S. Vanhove, S. Kieffer-Jaquinod, T.P. Rubio, et al., Antimicrobial histones and DNA traps in invertebrate immunity: evidences in *Crassostrea gigas*, J. Biol. Chem. 289 (2014) 24821–24831.

[56] C.T. Robb, E.A. Dyrynda, R.D. Gray, A.G. Rossi, V.J. Smith, Invertebrate extracellular phagocyte traps show that chromatin is an ancient defence weapon, Nat. Commun. 5 (2014) 4627.

[57] N. Sathyan, R. Philip, E.R. Chaithanya, P.R. Anil Kumar, S.P. Antony, Identification of a histone derived, putative antimicrobial peptide Himanturin from round whip ray *Himantura pastinacoides* and its phylogenetic significance, Results Immunol. 2 (2012) 120–124.

[58] C.B. Park, H.S. Kim, S.C. Kim, Mechanism of action of the antimicrobial peptide buforin II: buforin II kills microorganisms by penetrating the cell membrane and inhibiting cellular functions, Biochem. Biophys. Res. Commun. 244 (1998) 253–257.

[59] M. Dathe, T. Wieprecht, Structural features of helical antimicrobial peptides: their potential to modulate activity on model membranes and biological cells, Biochim. Biophys. Acta 1462 (1999) 71–87.

[60] A. Giangaspero, L. Sandri, A. Tossi, Amphipathic alpha helical antimicrobial peptides, Eur. J. Biochem. FEBS 268 (2001) 5589–5600.

[61] L.T. Nguyen, E.F. Haney, H.J. Vogel, The expanding scope of antimicrobial peptide structures and their modes of action, Trends Biotechnol. 29 (2011) 464–472.

[62] Y.S. Koo, J.M. Kim, I.Y. Park, B.J. Yu, S.A. Jang, K.S. Kim, et al., Structure-activity relations of parasin I, a histone H2A-derived antimicrobial peptide, Peptides 29 (2008) 1102–1108.

[63] M.E. Bustillo, A.L. Fischer, M.A. LaBouyer, J.A. Klaips, A.C. Webb, D.E. Elmore, Modular analysis of hipposin, a histone-derived antimicrobial peptide consisting of membrane translocating and membrane permeabilizing fragments, Biochim. Biophys. Acta 1838 (2014) 2228–2233.

[64] K. Matsuzaki, K. Sugishita, M. Harada, N. Fujii, K. Miyajima, Interactions of an antimicrobial peptide, magainin 2, with outer and inner membranes of Gram-negative bacteria, Biochim. Biophys. Acta 1327 (1997) 119–130.

[65] J. Xie, Y. Gou, Q. Zhao, K. Wang, X. Yang, J. Yan, et al., Antimicrobial activities and membrane-active mechanism of CPF-C1 against multidrug-resistant bacteria, a novel antimicrobial peptide derived from skin secretions of the tetraploid frog *Xenopus clivii*, J. Pept. Sci. Off. Publ. Eur. Pept. Soc. 20 (2014) 876–884.

[66] D.L. Evans, H. Kaur, J. Leary 3rd, K. Praveen, L. Jaso-Friedmann, Molecular characterization of a novel pattern recognition protein from nonspecific cytotoxic cells: sequence analysis, phylogenetic comparisons and antimicrobial activity of a recombinant homologue, Dev. Comp. Immunol. 29 (2005) 1049–1064.

[67] G. Aung, F. Niyonsaba, H. Ushio, N. Kajiwara, H. Saito, S. Ikeda, et al., Catestatin, a neuroendocrine antimicrobial peptide, induces human mast cell migration, degranulation and production of cytokines and chemokines, Immunology 132 (2011) 527–539.

[68] M. Yoshioka, N. Fukuishi, Y. Kubo, H. Yamanobe, K. Ohsaki, Y. Kawasoe, et al., Human cathelicidin CAP18/LL-37 changes mast cell function toward innate immunity, Biol. Pharm. Bull. 31 (2008) 212–216.

[69] L.O. Brandenburg, S. Jansen, C.J. Wruck, R. Lucius, T. Pufe, Antimicrobial peptide rCRAMP induced glial cell activation through P2Y receptor signalling pathways, Mol. Immunol. 47 (2010) 1905–1913.

[70] P. Peter Chiou, J. Khoo, N.C. Bols, S. Douglas, T.T. Chen, Effects of linear cationic alpha-helical antimicrobial peptides on immune-relevant genes in trout macrophages, Dev. Comp. Immunol. 30 (2006) 797–806.

[71] X. Tang, D. Metzger, S. Leeman, S. Amar, LPS-induced TNF-alpha factor (LITAF)-deficient mice express reduced LPS-induced cytokine: evidence for LITAF-dependent LPS signaling pathways, Proc. Natl. Acad. Sci. U. S. A. 103 (2006) 13777–13782.

[72] X.Z. Shi, R.R. Zhang, Y.P. Jia, X.F. Zhao, X.Q. Yu, J.X. Wang, Identification and molecular characterization of a Spatzle-like protein from Chinese shrimp (*Fenneropenaeus chinensis*), Fish Shellfish Immunol. 27 (2009) 610–617.

[73] C. Parthier, M. Stelter, C. Ursel, U. Fandrich, H. Lilie, C. Breithaupt, et al., Structure of the Toll-Spatzle complex, a molecular hub in Drosophila development and innate immunity, Proc. Natl. Acad. Sci. U. S. A. 111 (2014) 6281–6286.

[74] H.S. Lee, C.B. Park, J.M. Kim, S.A. Jang, I.Y. Park, M.S. Kim, et al., Mechanism of anticancer activity of buforin IIb, a histone H2A-derived peptide, Cancer Lett. 271 (2008) 47–55.

[75] M. Rose-Martel, M.T. Hincke, Antimicrobial histones from chicken erythrocytes bind bacterial cell wall lipopolysaccharides and lipoteichoic acids, Int. J. Antimicrob. Agents 44 (2014) 470–472.

[76] E.R. Chaithanya, R. Philip, N. Sathyan, P.R.A. Kumar, Molecular characterization and phylogenetic analysis of a histone-derived antimicrobial peptide teleostin from the marine teleost fishes, *Tachysurus jella* and *Cynoglossus semifasciatus*, ISRN Mol. Biol. 2013 (2013) 1–6.

[77] N. Sathyan, R. Philip, E.R. Chaithanya, P.R.A. Kumar, Identification and molecular characterization of molluskin, a histone-H2A-derived antimicrobial peptide from molluscs, ISRN Mol. Biol. 2012 (2012) 1–6.

[78] N. Sathyan, R. Philip, E.R. Chaithanya, P.R.A. Kumar, S.P. Antony, I.S.B. Singh, Identification of a histone derived, putative antimicrobial peptide sunettin from marine clam Sunetta scripta, Blue Biotechnol. J. 1 (2012) 397–403.

[79] N. Sathyan, R. Philip, E.R. Chaithanya, P.R.A. Kumar, V.N. Sanjeevan, I.S.B. Singh, Characterization of Histone H2A derived antimicrobial peptides, Harriottins, from sicklefin chimaera *Neoharriotta pinnata* (Schnakenbeck, 1931) and its evolutionary divergence with respect to CO1 and Histones H2A, ISRN Mol. Biol. 2013 (2013) 1–10.